



Poroelectric analysis of bone tissue differentiation by using the boundary element method

Y. González^{a,*}, M. Cerrolaza^a, C. González^b

^a Instituto Nacional de Bioingeniería, Facultad de Ingeniería, Universidad Central de Venezuela, Caracas, Venezuela

^b Servicio de Traumatología y Ortopedia, Hospital Universitario de Caracas, Caracas, Venezuela

ARTICLE INFO

Article history:

Received 25 February 2008

Accepted 22 September 2008

Available online 29 November 2008

Keywords:

Bone healing

Tissue differentiation

Boundary element method

Poroelectricity

Axi-symmetry

ABSTRACT

Fracture healing is initiated and tightly regulated mainly by growth factors and by mechanical environment around the callus site. Biomechanics of fracture healing have been previously studied. Most computational models are based on finite elements and some of them study the level of strain or stress in the different tissues. These strain/stress fields are the main mechanical stimuli affecting cell differentiation and ossification pathway. In this work, we incorporated that hypothesis into a poroelectric axi-symmetric boundary element callus model, where the pore pressure was included as a part of the stimuli function. This analysis allowed us to extend the observations made by other authors and a new poroelectric correlation between mechanical conditions and local tissue formation is proposed. This work shows the capability of the boundary element method to characterize the tissue phenotypes during a progressive healing process. The results were in good agreement with those reported in previous works.

© 2008 Elsevier Ltd. All rights reserved.

1. Introduction

1.1. Bone healing and tissue regeneration

Once a fracture occurs, a very complex process is auto-activated naturally to repair the injury. Fracture healing involves the generation of intermediate tissues, such as fibrous connective tissue, cartilage and woven bone, before final bone healing can occur, with different paths being governed by a variety of stimulating agents like the mechanical environment, hormonal and physiological patterns, geometric configuration of the fracture fragments and growth factors [1].

We can differentiate between primary or secondary fracture healing. However, most cases, which involve moderate gap sizes and fracture stability, heal by secondary fracture healing forming a voluminous callus. This type of healing benefits from a certain amount of inter-fragmentary movement (IFM) at the fracture site and has a series of sequential stages than can overlap to a certain extent, including inflammation, callus differentiation, ossification and remodelling. Bone ossification can occur mainly by endochondral and intramembranous ossification. In the first, cartilage is formed, calcified and replaced by bone. In the second, bone is

formed directly by osteoblasts. As depicted in Fig. 1, the process involves the coordinated participation of migration, differentiation and proliferation of inflammatory cells, angioblasts, fibroblasts, chondroblasts and osteoblasts which synthesize and release bioactive substances of extracellular matrix components (e.g., different types of collagen and growth factors).

Healing begins as undifferentiated mesenchymal cells migrating from the surroundings to produce initial connective tissue around the fracture site, forming an initial stabilizing callus. These cells proliferate and migrate from the surrounding soft tissue.

In the next stage, the localized differentiation of the mesenchymal cells into cartilage and bone forming cells leads to the production of cartilage and bone tissue in the callus (see Fig. 2), depending on the biological and mechanical conditions. These differentiated cells begin to synthesize the extracellular matrix of their corresponding tissue. Intramembranous woven bone is produced by direct differentiation of the stem cells into osteoblasts and appears adjacent to each side of the gap site, advancing to the center of the callus. At the same time, at the center of the callus, cartilage is formed by chondrogenesis (Fig. 2), except right beside the gap where the stability is still very small and high relative displacement prevents the differentiation of mesenchymal cells.

Once the callus is filled (mainly by cartilage), endochondral ossification begins following a complex sequence of cellular events including cartilage maturation and degradation, vascularity and osteogenesis. The ossification continues until all the

* Corresponding author. Tel.: +58 212 8384868, +58 212 6051750/1751; fax: +58 212 6053115.

E-mail address: yomar.gonzalez@inabio.edu.ve (Y. González).

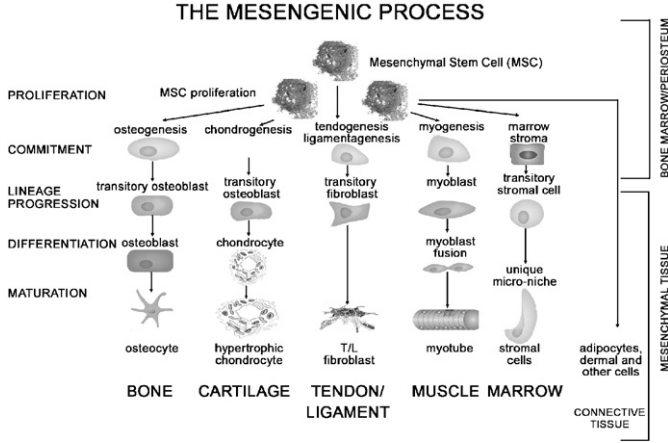


Fig. 1. The mesengenic process [3].

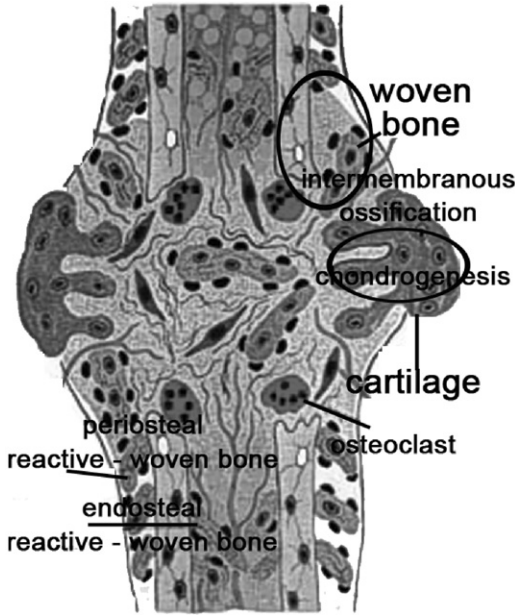


Fig. 2. Callus phenotype at day 9 after fracture. Notice the intramembranous ossification process close to the periosteum and the chondrogenesis present in most of fracture site [4].

cartilage has been replaced by bone and a bony bridge surrounds the fracture gap, achieving a good stabilization and sufficient stiffness. When the fracture is completely stabilized, mesenchymal cells start to invade the gap. Once the gap has ossified, remodelling of the fracture site begins gradually in order to restore the original internal structure and shape [2].

1.2. Boundary element framework

The boundary element method has recently been widely applied in simulation of biological problems. A few interesting works have been published illustrating the versatility of the method in this area [5–7].

The advantages below are believed to support the applicability of the method as a framework for bone healing simulation.

- High accuracy can be expected at the boundaries, internal points and interfaces from the strain/stress field magnitudes [5].
- Multi-domain capability [8].

- A generalized boundary integral equation for non-homogeneous isotropic media [9] can be applied within each region with spatially varying material properties.
- The BEM distinguishes itself as a boundary method, meaning that the numerical discretization is conducted at reduced spatial dimension [10].
- Remeshing is no longer needed to update callus size and shape.
- Kernels for time dependent analysis of diffusion and particles migration problems are available [11,12].
- No-symmetric boundary conditions have been incorporated into recent axi-symmetric kernels [13].
- Displacements and tractions at the boundaries can be calculated simultaneously.

The aim is therefore to establish BEM as an attractive alternative to the more familiar finite difference and finite element methods to characterize the strain/stress environment at appropriate locations within callus. The poroelastic code presented is part of a set of BEM codes needed to establish a dynamic callus growth model. All results were in good agreement with those reported in previous works, highlighting the potential of the axi-symmetric multi-region code to establish the mechanical stimuli associated with a specific tissue phenotype.

The BEM code contains the axi-symmetric fundamental solutions for steady-state poroelastic problems in a linear-elastic, isotropic and non-homogeneous media, following the Biot consolidation theory [14].

The constitutive equations for three-dimensional consolidation, written in the Cartesian form are

$$(\lambda + \mu)u_{i,j,j} + \mu u_{i,j,j} - \beta p_{,i} + f_i = 0 \quad (1)$$

$$k p_{,ij} - \left(\frac{\beta^2}{\lambda_u - \lambda} \right) \dot{p} - \beta \dot{u}_{i,j} + \psi = 0 \quad (2)$$

where u_i represents the displacement, p is the excess pore pressure, f_i is the body force per unit volume, and ψ is the time rate of volumetric fluid supply per unit volume. Meanwhile, λ and μ are the drained Lamé elastic constants, λ_u is the undrained elastic modulus, k is the permeability and β is a function of B , called the compressibility coefficient or Skempton pore pressure coefficient.

The uncoupled poroelastic boundary integral equation for axi-symmetric bodies follows the matrix form (3). The generalized quasi-static displacements and tractions are transformed into a cylindrical coordinate system (r, φ, z) and then circumferential integration is performed. [15,16]

$$\begin{bmatrix} C_{rr}(P) & C_{rz}(P) & C_{r\theta}(P) \\ C_{zr}(P) & C_{zz}(P) & C_{z\theta}(P) \\ C_{\theta r}(P) & C_{\theta z}(P) & C_{\theta\theta}(P) \end{bmatrix} \begin{bmatrix} U_r(P) \\ U_z(P) \\ \theta(P) \end{bmatrix} = 2\pi \int_{\Gamma} \begin{bmatrix} U_{rr}^*(P, Q) & U_{rz}^*(P, Q) & U_{r\theta}^*(P, Q) \\ U_{zr}^*(P, Q) & U_{zz}^*(P, Q) & U_{z\theta}^*(P, Q) \\ U_{\theta r}^*(P, Q) & U_{\theta z}^*(P, Q) & U_{\theta\theta}^*(P, Q) \end{bmatrix} \begin{bmatrix} T_r(Q) \\ T_z(Q) \\ q(Q) \end{bmatrix} r(Q) d\Gamma - 2\pi \int_{\Gamma} \begin{bmatrix} T_{rr}^*(P, Q) & T_{rz}^*(P, Q) & T_{r\theta}^*(P, Q) \\ T_{zr}^*(P, Q) & T_{zz}^*(P, Q) & T_{z\theta}^*(P, Q) \\ T_{\theta r}^*(P, Q) & T_{\theta z}^*(P, Q) & T_{\theta\theta}^*(P, Q) \end{bmatrix} \begin{bmatrix} U_r(Q) \\ U_z(Q) \\ \theta(Q) \end{bmatrix} r(Q) d\Gamma \quad (3)$$

P is the field point, Q is the integration point, $C_{\alpha\beta}(P)$ is the free term, $r(Q)$ is the radial coordinate of Q , U_r and U_z are the displacements in radial and axial direction, respectively, θ is now called the excess pore pressure, T_r and T_z are the tractions in radial and axial direction, respectively. $U_{rr}^*(P, Q)$, $U_{rz}^*(P, Q)$, $U_{r\theta}^*(P, Q)$, $U_{zr}^*(P, Q)$, $U_{zz}^*(P, Q)$, $U_{z\theta}^*(P, Q)$, $T_{rr}^*(P, Q)$, $T_{rz}^*(P, Q)$, $T_{r\theta}^*(P, Q)$ and $T_{zz}^*(P, Q)$ are the kernel

Download English Version:

<https://daneshyari.com/en/article/513161>

Download Persian Version:

<https://daneshyari.com/article/513161>

[Daneshyari.com](https://daneshyari.com)